Original Manuscript

JOURNAL OF COMPOSITE MATERIALS

Journal of Composite Materials
2025, Vol. 0(0) 1–7

DOI: 10.1177/00219983251363755
journals.sagepub.com/home/jcm
Sage

On the relationship between non-linearity and initial stiffness in PAN-based carbon fibers

Riley Perez[1,*], Seth A. Hill[1,*], Vasco Pereira[1] and Francisco López Jiménez[1]

Abstract

The longitudinal tensile behavior of carbon fibers is studied to characterize the relationship between initial stiffness and their non-linear behavior. Four different PAN-based fibers are measured through single fiber tensile testing. The results show clear non-linear behavior for all fibers, with a significant correlation between the non-linearity and the initial stiffness of the fibers. These relationships are quantified and the experiments are used to fit established models for the non-Hookean response of carbon fibers. We find a negative correlation between initial stiffness and non-linearity in the response.

Keywords

carbon fiber, single fiber, mechanical properties, non-linearity, non-Hookean elastic behavior, single-filament tensile test

Introduction

The nano-structure of carbon fiber consists of sheets of carbon atoms, which depending on the manufacturing process can be turbostratic, graphitic, or hybrid.[1,2] The mechanical properties of the fibers, and in particular their stiffness, depend not only on the stiffness of the carbon crystallites, but also their orientation: fibers in which the crystallite planes are well-aligned with the fiber direction are stiffer than fibers in which there is a wider distribution of orientations.[3–5]

Another important consequence of the internal structure of the fibers is that they are mechanically nonlinear[6–12]: they stiffen under tension and soften under compression. This is due to the graphite crystallites rotating as the fiber is loaded. As tensile loading is applied, they align with the fiber direction, increasing the stiffness, while compression results in softening.[13] The simplest description for the non-linear behavior of carbon fibers that is able to capture the behavior of most fibers is given by the empirical model:

$$\sigma = E_0(1+\gamma\varepsilon)\varepsilon \tag{1}$$

where σ is the stress, ε is the strain, E_0 is the initial stiffness, and γ is a parameter that describes the non-linearity of the fiber. This model was first proposed to capture the non-linearity of laminates[7,14] and subsequently applied to single fibers.[10] The limitation of this phenomenological model is that it does not connect the mechanical response to the microstructure of the fibers. Other phenomenological relationships for the behavior of single fibers have been developed, such as polynomial relationships based on strain energy density[9]:

$$E_1 = \frac{1}{S_{11} + 2S_{111}\sigma_1 + 3S_{1111}\sigma_1^2} \tag{2}$$

where E_1 is the non-linear Young's modulus and S_{11}, S_{111}, and S_{1111} are coefficients used to express the strain energy in the fiber as a quadratic function of the stresses.

A physically based model was presented by Northolt et al.,[15] which considered the reorientation of the crystalline nano-structure of the fibers. The stress σ and strain ε are related by:

$$\varepsilon = \frac{\sigma}{e_1} + <\cos^2\phi_0>\left(1-\exp\left(-\frac{\sigma}{g}\right)\right) \tag{3}$$

where e_1 is the modulus of carbon crystallites, g is the shear modulus between the carbon planes, and $<\cos^2\phi_0>$ is the second moment of the crystallite orientation

[1]Ann and H.J. Smead Department of Aerospace Engineering Sciences, University of Colorado Boulder, Boulder, CO, USA

*These authors contributed equally to this work.

Corresponding author:
Francisco López Jiménez, Ann and H.J. Smead Department of Aerospace Engineering Sciences, University of Colorado Boulder, 3775 Discovery Drive Boulder, Boulder, CO 80303, USA.
Email: francisco.lopezjimenez@colorado.edu

Data Availability Statement included at the end of the article

distribution before any load is applied. The initial stiffness is given by:

$$\frac{1}{E_0} = \frac{1}{e_1} + \frac{<\cos^2\phi_0>}{g} \tag{4}$$

Equation (3) can then be rewritten using initial stiffness instead of crystallite orientation as:

$$\varepsilon = \frac{\sigma}{e_1} + g\left(\frac{1}{E_0} - \frac{1}{e_1}\right)\left(1 - \exp\left(-\frac{\sigma}{g}\right)\right) \tag{5}$$

Other approaches explored in literature include array and mosaic models combining regions with different crystallite orientation[4] or Mori-Tanaka theory to model the fibers as a composite of crystallite and amorphous regions.[16]

The mechanical non-linearity of fibers is often ignored in the analysis and design of carbon fiber reinforced polymers. Instead, their stiffness is usually described solely by their axial Young's modulus, therefore assuming a linear relationship. However, fiber nonlinearity plays an important role in the case of High Strain Composites.[14,17–19] These are very thin laminates that achieve strains of over 2% under bending, due to shear stabilization of the microbuckling in the compression side, and which are important in the design of deployable space structures.[20–22] The non-linearity also plays an important role in the predictive modeling of failure micromechanics, such as kink band formation.[23,24] Furthermore, recent advances toward predicting composite failure focus on high fidelity finite element models,[25–27] where material non-linearities in fibers and matrix might play an important role.

A particularly unexplored aspect of the nano-structure of carbon fiber is the correlation between non-linearity and fiber stiffness for each individual fiber. Huang and Young showed that crystallite orientation is more pronounced in the case of fibers with lower modulus,[28] which aligns with the current understanding of the micromechanics of carbon fiber: in soft fibers the crystallites are initially less aligned, so there is more opportunity for stiffening as they align under loading. However, their study compared different types of fibers to each other, but did not explore differences between fibers of the same type. Kant and Penumadu[29] used dynamic mechanical characterization to measure the response of individual fibers from six different types of PAN fibers, showing opposite results, i.e. the same value of γ in equation (1) for a wide range of fiber elastic moduli. Other studies found in literature infer the value of γ from test at the coupon level,[14] so it is impossible to distinguish the behavior of each fiber.

Here, we perform tensile testing on single filaments, using four different types of PAN-based carbon fibers. The behavior of the each of the fibers is fitted to equations (1) and (3), and we explore the correlation between different parameters, as a way to rationalize the behavior of the fibers.

Experiments

We have tested single filaments to characterize the non-linearity of four different PAN-based fibers: three intermediate modulus fibers (IM7, MR60H, and IMS60) and one high modulus fiber (HS40). The experiments followed the ASTM D3379 standard[30] (retired, but with no replacement), in which single fibers are glued to a piece of paper used to mount them in a tensile machine. The gauge length is 30 mm and the fibers are loaded at a constant displacement rate of 0.2 mm/min, on an Instron 5969 with a 10 N load cell. Fibers with lengths ranging from 9.5 mm to 54 mm were used to calibrate the compliance of the system, which was assumed to be linear, constant, and the same for all fibers.

In order to ensure that the non-linearity explored in this work is not the effect of slippage or some source of friction, a small number of fibers were subjected to loading and unloading to increasing levels of stress, see Figure 1(a). These experiments show that the force-displacement curve follows the same path on subsequent runs, with no noticeable hysteresis or permanent deformation. Despite no visible effect of the unloading, the results from these cyclic tests are not included in the rest of the study, so that the conditions are the same for all samples. Figure 1(a) also shows the typical variations in initial stiffness, stiffness non-linearity, and strength that is observed between identical fibers.

The diameter of the fibers was not directly measured in order to minimize manipulation before mechanical testing, which could impact their stiffness and strength. Instead, the stress in the fibers is calculated from the force during the test using the nominal cross section, with the diameter provided by the manufacturer. The diameters used, as well as the numbers of fibers tested on each case, are provided in Table 1. The values of the diameter were verified through images taken with Scanning Electron Microscope on a small set of fibers, including cross-section and side views, see Figure 1(b)-(c). These fibers were not used in the mechanical testing. The micrographs showed that the cross sections are very close to an ideal cylinder, and that typical variations in fiber diameter are less than 5%, which would correspond to variations of less than 10% in fiber area.

Results

This section presents the experimental results, as well as analysis using the two constitutive modeling approaches presented in equations (1) and (5). Our goal is to explore the variations in non-linearity amongs fibers of the same type and between different types, as well the relationship with other mechanical parameters. In all cases, the test results are fitted to predictions using *fminsearch* in Matlab, reducing the difference between measured and predicted stress for all values of recorded strain in the experiment.

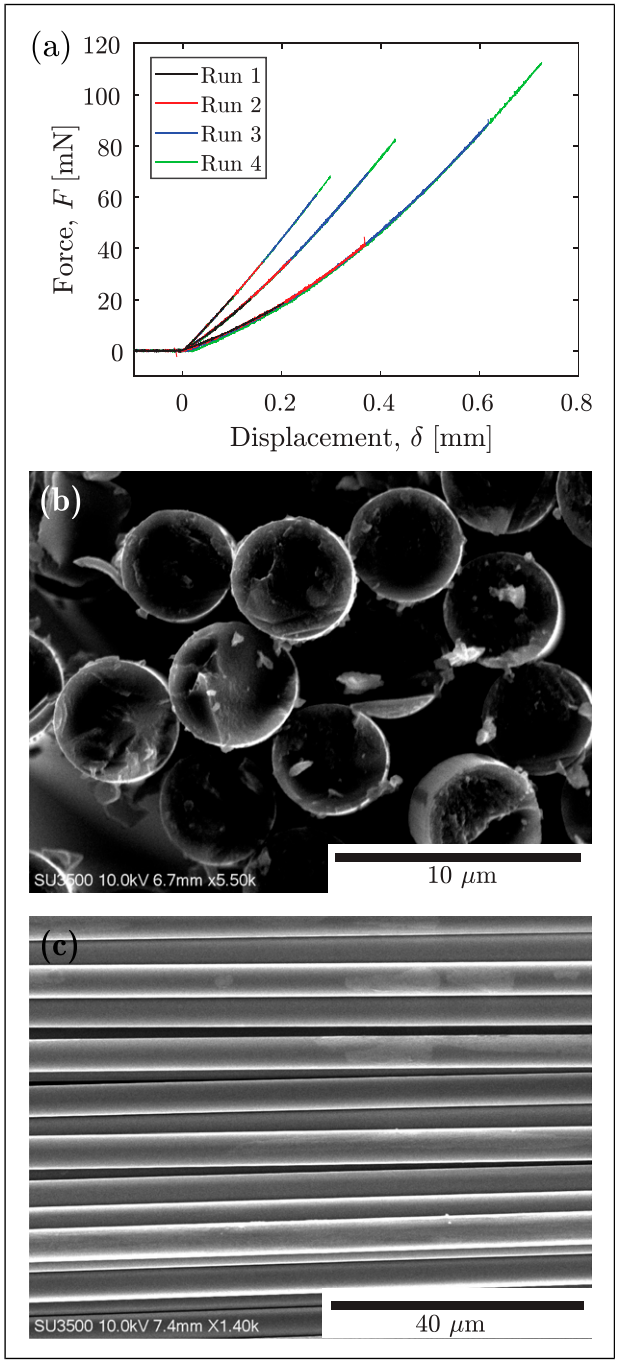

Figure 1. (a) Results of testing three IM7 fibers under loading and unloading to increasing maximum loads. (b) Cross-section and (c) side view of IM7 fibers under scanning electron microscope.

We start by fitting our experimental results to the empirical model in equation (1), where the main advantage is that the non-linearity is described by a single parameter, γ. This enables a straightforward comparison with other parameters, such as the initial stiffness.

Figure 2(a)shows the initial stiffness, E_0, versus the non-linear factor, γ, for all fibers tested. All fibers show a wide range of values for E_0, and an inverse relationship between initial stiffness and non-linearity, where fibers that are initially softer (low values of E_0) tend to stiffen more (high values of γ). This agrees with the proposed behavior at the nano-scale: soft fibers have crystallites that are less aligned with the fiber direction, and so they are able to stiffen significantly as they rotate under loading and align with the fiber direction. The figure also shows a linear fit for each kind of fiber, with results summarized in Table 2. The R^2 factors for all fittings are significant but relatively low, in the 0.33 to 0.69 range.

Table 1. Nominal modulus and diameters, as well as total number of fibers tested, for the four type of fibers considered in this study.

Fiber name	Modulus	Diameter	Tested
IM7 (Hexcel)	276 GPa	5.2 μm	108
MR60H (Mitsubishi)	280 GPa	5 μm	40
IMS60 (Teijin)	290 GPa	5 μm	40
HS40 (Mitsubishi)	425 GPa	5 μm	40

Figure 2(b) and (c) show the fiber strength, σ_f, and the energy absorbed during the test, calculated by integrating the force-displacement response, versus the non-linear factor for each fiber. We again observe a wide distribution of the values for all parameters, but in both cases case, we observe no relationship between the parameters. In particular, the values of $R^2 < 0.1$ for all the correlations shown in Figure 2(b)–(c), and so the values of the linear fit are not provided.

We further characterize the variation in fiber non-linearity by plotting the probability density function of the non-linear factor, γ, and the initial stiffness, E_0, see Figure 3. The distributions are similar for all intermediate modulus fibers (IM7, MR60H, IMS60), while the high modulus fiber (HS40) has generally higher values of both parameters. This observation agrees with the values reported in Table 2.

We now consider the model by Northolt et al.[15] We start by fitting the stress-strain response of each fiber to equation (5), where the free parameters are e_1, g, and E_0. In this case, the initial stiffness is obtained from the fitting, and not from the initial slope of the curve, but the values obtained are nearly identical. The results are shown in Figure 4, as a function of the initial stiffness E_0. The second moment of the crystalline orientation, $<\cos^2\phi_0>$, is calculated using equation (4). The results omit five outliers that provided unrealistic results of the parameters (e.g., values of e_1 in the order of 10^5 GPa). These are the result of fibers with almost perfectly linear stiffness, which is hard to capture with equation (5).

The results show correlation between the in-plane modulus of the graphitic plane, e_1, and the initial fiber stiffness, E_0. In the case of intermediate modulus fibers, a similar relationship is observed for the shear stiffness

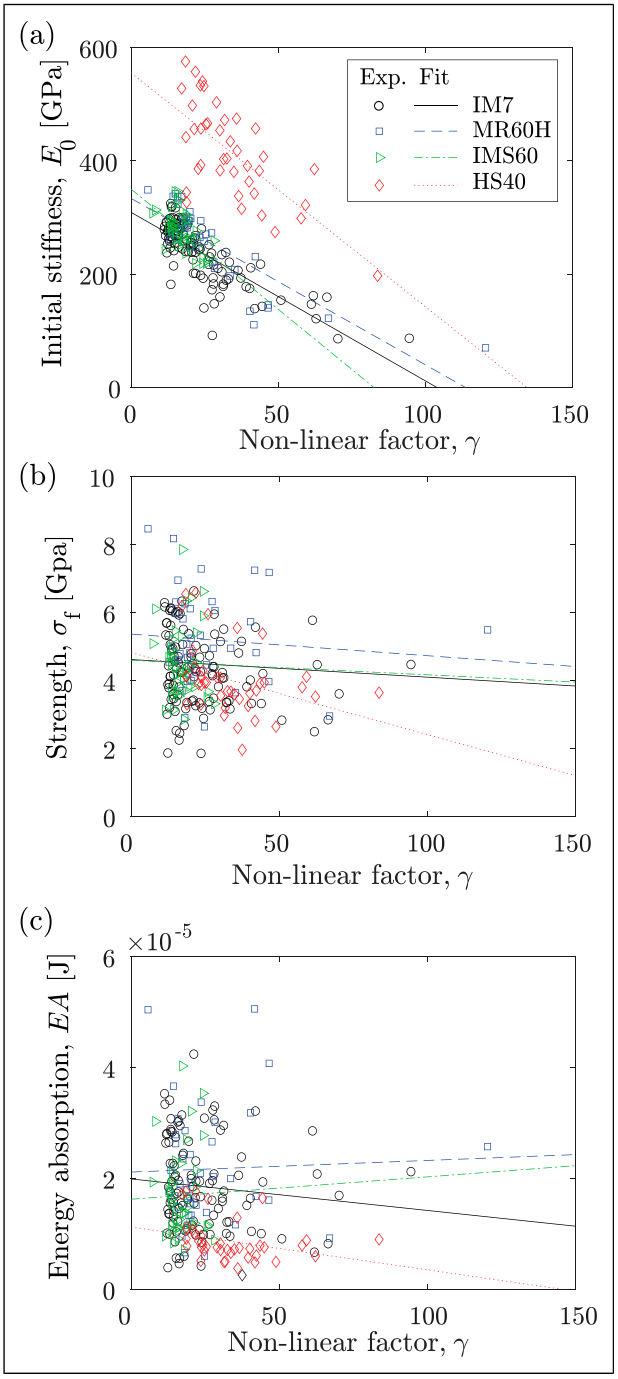

Figure 2. (a) Initial stiffness, E_0, (b) strength, σ_f, and (c) energy absorbed during tensile test, versus the no-linear factor γ, for all four types of PAN-based fibers. The legend applies to all figures.

between the planes, g, although with a weaker correlation. The high modulus fibers, HS40, do not follow this behavior, and have a similar range of values of g (between 1 and 3 GPa for most fibers), despite their higher modulus. This agrees with the higher value of γ for HS40 reported in Table 2, since lower shear stiffness means that the crystallite planes can rearrange more easily.

Table 2. Parameters obtained fitting experimental results to equation (1). Each fiber is fitted individually, and the results are reported as mean ± standard deviation. The coefficient of determination R^2 of the fitting is provided.

Fiber name	E_0 (GPa)	Γ	Fit (E_0 in GPa)	R^2
IM7	237 ± 53	24.0 ± 14.3	$E_0 = -3.0\gamma + 309.2$	0.63
MR60H	255 ± 68	26.6 ± 19.3	$E_0 = -2.9\gamma + 333.7$	0.69
IMS60	277 ± 33	17.1 ± 4.5	$E_0 = -4.2\gamma + 350.1$	0.33
HS40	415 ± 85	34.0 ± 14.1	$E_0 = -4.1\gamma + 555.3$	0.47

The values reported in Figure 4 show a significant spread, which is in part attributed to the fact that the equation (5) has three parameters to be fit (e_1, g, and E_0), as opposed to just two for equation (1) The results contradict the expectation that fibers of the same type will have similar values of the microstructure stiffness parameters e_1 and g. In order to explore this possibility, we fit all experiments from the same type of fiber together. This means, the variables that we fit

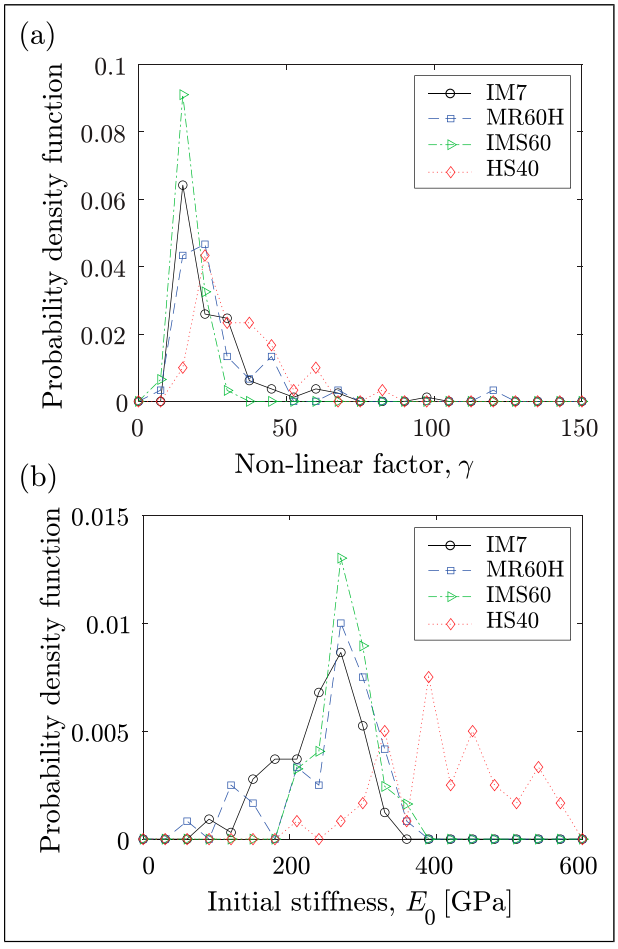

Figure 3. Probability density function of the non-linear factor, γ, and the initial stiffness, E_0, for the four types of PAN-based fibers.

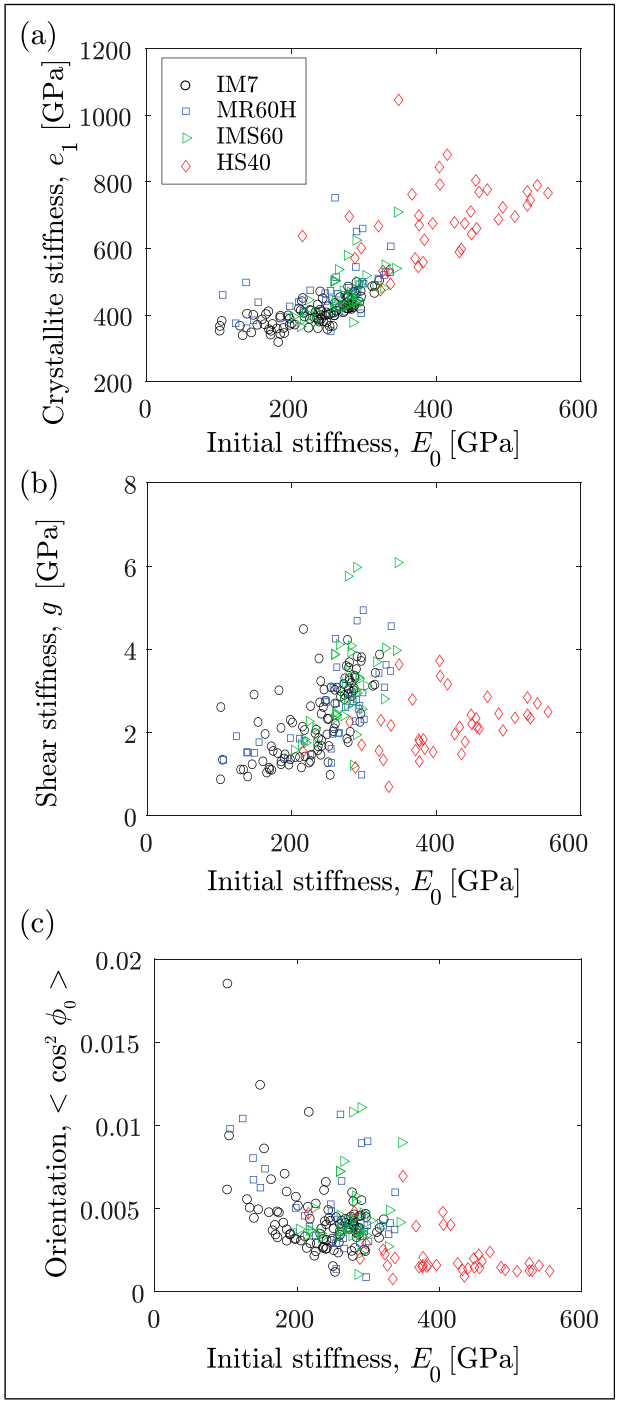

Figure 4. (a) Crystallite stiffness, e_1, (b) shear stiffness between planes, g, and (c) second moment of the crystallite orientation distribution, versus the initial stiffness E_0, for all four types of PAN-based fibers. The legend applies to all figures.

are the values of e_1 and g, common for all fibers, as well as a different value of E_0 (which can be related to the value of $<\cos^2\phi_0>$) for each individual fiber. The results of this fit, as well as those obtained previously, are reported in Table 3. The values of all parameters obtained fitting all fibers together are slightly lower than the average of the values obtained by fitting the fibers individually. Both of them are also lower than theoretical predictions reported in literature, but with a similar order of magnitude. For example, it is estimated that e_1 lies in the 650 to 1200 GPa, and g between 5 and 15 GPa.[15,18,31–33]

Discussion and conclusions

We have used tensile testing on single fibers to characterize the behavior of different PAN-based carbon fibers. Our results show a negative correlation between initial stiffness and non-linearity within the same fiber type: initially soft fibers stiffen as the fibers are strained, while initially stiff fibers show little variation in stiffness. This agrees with the hypothesis that stiffness is largely dominated by the orientation of the carbon crystallites, which rotate and realign with the fiber direction when load is applied. It is important to note that this relationship does not apply between fibers of different types: the high modulus fibers HS40 exhibit both higher stiffness and higher non-linearity than all the intermediate fibers tested. Our experiments did not measure fiber microstructure, and efforts to fit our results to existing models for this proposed mechanism were inconclusive. Previous experiments directly measuring the orientation distribution of the crystallites through X-ray diffraction have shown that it correlates with the non-linearity parameter γ.[13] It has also been shown that the stiffness of fibers correlates to their radius, decreasing as radius increases,[34] which can be attributed to different properties on the outer and inner regions of the fiber. However, studies with direct observation of the fiber microstructure are usually limited in the number of fibers, due to experimental complexity.

Kant and Penumadu[29] used an alternative method, superimposing small amplitude harmonic loads onto the monotonic loading of quasi-static tensile tests. This provides storage and loss modulus as a function of the global strain of the single fiber and is intended to remove the effect of the system compliance in all experiments, instead of applying the same value to all experiments. They found that the ratio of γE_0 to E_0 is equal to 29.4 for a wide range of PAN fibers, including both intermediate and high modulus fibers. However, their results show an increase in compliance of the testing setup as the load increases, which they attribute to delamination between fiber and glue. This is in disagreement with our observation that the load-displacement behavior is fully reversible even for high loads. The same technique, combined with wide- and small-angle scattering to measure the orientation and size of amorphous regions, suggests that the non-linearity in the fiber stiffness is a result of elastic planar motion within regions of turbostratic carbon.[35]

The discrepancy between different experiments and models found in literature, including the present study, highlight the need for further characterization of the tensile properties of carbon fiber. While these tests are routinely

Table 3. Parameters obtained fitting experimental results to equation (5). In the case of parameters that vary from fiber to fiber, the results are reported as mean ± standard deviation.

	Individual fit			Combined fit		
Fiber name	e_1 (GPa)	g (GPa)	$<\cos^2\phi_0>$	e_1 (GPa)	g (GPa)	$<\cos^2\phi_0>$
IM7	409 ± 39	2.3 ± 0.9	0.0043 ± 0.0022	355.5	1.3	0.0023 ± 0.0021
MR60H	476 ± 82	2.5 ± 1.0	0.0049 ± 0.0024	375.0	1.0	0.0018 ± 0.0022
IMS60	468 ± 71	3.1 ± 1.2	0.0046 ± 0.0022	444.3	2.8	0.0039 ± 0.0013
HS40	684 ± 114	2.2 ± 0.7	0.0022 ± 0.0013	659.4	2.0	0.0020 ± 0.0012

performed to obtain their failure properties,[36–39] there are relatively less studies addressing nonlinearity. In particular, there is a need for new techniques able to characterize both the macroscopic response (force vs displacement) as well as local properties (local strain, radius, crystallite orientation) for a large number of fibers, as well as models making use of the results of such experiments.

Acknowledgements

We thank Dr Tomoko Borsa (Colorado Shared Instrumentation in Nanofabrication and Characterization, CU Boulder) for help with the Scanning Electron Microscope.

ORCID iD

Francisco López Jiménez https://orcid.org/0000-0002-8082-7221

Funding

The authors disclosed receipt of the following financial support for the research, authorship, and/or publication of this article: Funding from Redwire Space (formerly Roccor, at the time of the research), through the Air Force Research Lab Small Business Technology Transfer (STTR) Program, contracts FA9453-17-P-0463 and FA9453-19-C-0597, is gratefully acknowledged. Seth Hill and Riley Perez were also supported by the Discovery Learning Apprenticeship program at the University of Colorado Boulder.

Declaration of conflicting interests

The authors declared no potential conflicts of interest with respect to the research, authorship, and/or publication of this article.

Data Availability Statement

Data is available in the fig Share repository https://doi.org/10.6084/m9.figshare.29363210.[40]

References

1. Oberlin A. Carbonization and graphitization. *Carbon* 1984; 22(6): 521–541.
2. Johnson D. Structure-property relationships in carbon fibres. *J Phys D Appl Phys* 1987; 20(3): 286–291.
3. Huang Y and Young R. Effect of fibre microstructure upon the modulus of pan-and pitch-based carbon fibres. *Carbon* 1995; 33(2): 97–107.
4. Shioya M, Hayakawa E and Takaku A. Non-hookean stress-strain response and changes in crystallite orientation of carbon fibres. *J Mater Sci* 1996; 31(17): 4521–4532.
5. Loidl D, Peterlik H, Müller M, et al. Elastic moduli of nanocrystallites in carbon fibers measured by in-situ x-ray microbeam diffraction. *Carbon* 2003; 41(3): 563–570.
6. Curtis G, Milne J and Reynolds W. Non-hookean behaviour of strong carbon fibres. *Nature* 1968; 220(5171): 1024–1025.
7. Van Dreumel WH and Kamp JL. Non hookean behaviour in the fibre direction of carbon-fibre composites and the influence of fibre waviness on the tensile properties. *J Compos Mater* 1977; 11(4): 461–469.
8. Beetz CP Jr and Budd G. Strain modulation measurements of stiffening effects in carbon fibers. *Rev Sci Instrum* 1983; 54(9): 1222–1226.
9. Ishikawa T, Matsushima M and Hayashi Y. Hardening non-linear behaviour in longitudinal tension of unidirectional carbon composites. *J Mater Sci* 1985; 20(11): 4075–4083.
10. Hughes J. Strength and modulus of current carbon fibres. *Carbon* 1986; 24(5): 551–556.
11. Kowalski I. Characterizing the tensile stress-strain nonlinearity of polyacrylonitrile-based carbon fibers. *Composite materials: testing and design (eighth conference)*. ASTM International.
12. Ueda M, Saito W, Imahori R, et al. Longitudinal direct compression test of a single carbon fiber in a scanning electron microscope. *Compos Appl Sci Manuf* 2014; 67: 96–101.
13. Djordjevic IM, Sekulić DR and Stevanović MM. Non-linear elastic behaviour of carbon fibres of different structural and mechanical characteristic. *J Serb Chem Soc* 2007; 72(5): 513–521.
14. Murphey TW, Peterson ME and Grigoriev MM. Large strain four-point bending of thin unidirectional composites. *J Spacecraft Rockets* 2015; 52(3): 882–895.
15. Northolt M, Veldhuizen L and Jansen H. Tensile deformation of carbon fibers and the relationship with the modulus for shear between the basal planes. *Carbon* 1991; 29(8): 1267–1279.
16. Tanaka F, Okabe T, Okuda H, et al. The effect of nanostructure upon the deformation micromechanics of carbon fibres. *Carbon* 2013; 52: 372–378.
17. Tsuji N and Kubomura K. Non-linear compression stress-strain curve of pitch-based high modulus carbon fibre

composites and structural responses. *J Mater Sci* 1992; 27: 3782–3788.
18. Schlothauer A, Pappas GA and Ermanni P. Material response and failure of highly deformable carbon fiber composite shells. *Compos Sci Technol* 2020; 199: 108378.
19. Harihara Sharma A, Rose TJ, Bearns N, et al. Analysis of geometric and material nonlinearity in the column bending test. *AIAA J* 2024; 62(4): 1300–1310.
20. Murphey TW, Francis W, Davis B, et al. High strain composites. *2nd AIAA spacecraft structures conference*, p. 0942.
21. Echter MA, Gillmer SR, Silver MJ, et al. A multifunctional high strain composite (hsc) hinge for deployable in-space optomechanics. *Smart Mater Struct* 2020; 29(10): 105010.
22. Dharmadasa BY, Mejia-Ariza JM, Arya M, et al. Design of flexures for deployable reflectarrays using high strain composites. *AIAA scitech 2022 Forum*, p. 0651.
23. Yokozeki T, Ogasawara T and Ishikawa T. Effects of fiber nonlinear properties on the compressive strength prediction of unidirectional carbon–fiber composites. *Compos Sci Technol* 2005; 65(14): 2140–2147.
24. Yokozeki T, Ogasawara T and Ishikawa T. Nonlinear behavior and compressive strength of unidirectional and multidirectional carbon fiber composite laminates. *Compos Appl Sci Manuf* 2006; 37(11): 2069–2079.
25. Swolfs Y, Verpoest I and Gorbatikh L. A review of input data and modelling assumptions in longitudinal strength models for unidirectional fibre-reinforced composites. *Compos Struct* 2016; 150: 153–172.
26. López Jiménez F. Numerical modeling of stress concentration around failed fibers in unidirectional composites. *AIAA Scitech 2021 Forum*, p. 0087.
27. Breite C, Melnikov A, Turon A, et al. Detailed experimental validation and benchmarking of six models for longitudinal tensile failure of unidirectional composites. *Compos Struct* 2022; 279: 114828.
28. Huang Y and Young R. Non-linear elasticity in carbon fibres. *J Mater Sci Lett* 1993; 12(2): 92–95.
29. Kant M and Penumadu D. Dynamic mechanical characterization for nonlinear behavior of single carbon fibers. *Compos Appl Sci Manuf* 2014; 66: 201–208.
30. *ASTM D3379. Standard test method for tensile strength and Young's modulus for high-modulus single-filament materials*. West Conshohocken, PA: ASTM International, 1989.
31. Blakslee O, Proctor D, Seldin E, et al. Elastic constants of compression-annealed pyrolytic graphite. *J Appl Phys* 1970; 41(8): 3373–3382.
32. Nicklow R, Wakabayashi N and Smith H. Lattice dynamics of pyrolytic graphite. *Phys Rev B* 1972; 5(12): 4951–4962.
33. Gillis PP. Calculating the elastic constants of graphite. *Carbon* 1984; 22(4-5): 387–391.
34. Mesquita F, Bucknell S, Leray Y, et al. Single carbon and glass fibre properties characterised using large data sets obtained through automated single fibre tensile testing. *Compos Appl Sci Manuf* 2021; 145: 106389.
35. Meek N and Penumadu D. Nonlinear elastic response of pan based carbon fiber to tensile loading and relations to microstructure. *Carbon* 2021; 178: 133–143.
36. Pardini LC and Manhani LGB. Influence of the testing gage length on the strength, young's modulus and weibull modulus of carbon fibres and glass fibres. *Math Res* 2002; 5: 411–420.
37. Kim J, McDonough WG, Blair W, et al. The modified-single fiber test: a methodology for monitoring ballistic performance. *J Appl Polym Sci* 2008; 108(2): 876–886.
38. López Jiménez F and Pellegrino S. Failure of carbon fibers at a crease in a fiber-reinforced silicone sheet. *J Appl Mech* 2013; 80(1): 011020.
39. Mesquita F, Bucknell S, Leray Y, et al. Large datasets of single carbon and glass fibre mechanical properties obtained with automated testing equipment. *Data Brief* 2021; 36: 107085.
40. Lopez Jimenez F. On the relationship between non-linearity and initial stiffness in PAN-based carbon fibers. Epub ahead of print 19 June 2025. DOI: 10.6084/m9.figshare.29363210.v1.